

K_{β}/K_{α} X-Ray Intensity Ratios for Cr, Mn, Fe, and Co Excited by 8.735 keV Energy

R. YILMAZ*

Department of Physics, Faculty of Sciences, Yüzüncü Yıl University, Van, Turkey

(Received June 14, 2017; in final form January 8, 2018)

In this study, the K shell intensity ratios K_{β}/K_{α} have been experimentally determined for the elements Cr, Mn, Fe, and Co. Measurements have been carried out at 8.735 keV excitation energy by using secondary excitation method. K X-rays emitted by samples have been counted by a Si (Li) detector with 160 eV resolutions at 5.9 keV. The measured values were compared with the calculated theoretical values. The obtained values are in good agreement with the calculated values.

DOI: [10.12693/APhysPolA.133.1227](https://doi.org/10.12693/APhysPolA.133.1227)

PACS/topics: K X-ray intensity ratios, X-ray fluorescence, cross-sections

1. Introduction

K X-ray intensity ratios and K shell X-ray production cross-sections are important for non-destructive trace element analysis using energy-dispersive XRF in various phenomena in the fields of atomic and nuclear physics. In the X-ray analytical methods, an energetic beam of primary radiation hits the sample, causes primary ionizations in different inner shells of the atoms. De-excitation of the atom from the ionized state emits characteristic X-ray line which is used for analysis. The measurements of K_{β}/K_{α} intensity ratios are important for comparison with theoretical predictions based on the atomic models in order to test the validity of these models. The K_{α} X-rays arise from the L - to the K shell transitions. The K_{β} X rays arise from the M -, N -, O -, etc. to the K -shell transitions.

In recent years, there are theoretical models based on the result of multi-configuration Dirac-Fock (MCDF) calculations, on the K X-ray intensities, for reliable descriptions of very complex X-ray spectra of multiply ionized atoms [1–3]. Polasik has theoretically determined influence of changes in the valence electronic configuration on the K_{β} -to- K_{α} X-ray intensity ratios of the $3d$ transition metals [4]. The study of Polasik is based on MCDF and the Coulomb and Babushkin gauges [5, 6]. There are especially important studies of the K_{β}/K_{α} X-ray intensity ratios for $3d$ transition elements by Raj et al. and Pawlowski [7–13].

Also, there have been various investigations on K X-ray fluorescence cross-sections and intensity ratios. Ertuğrul et al. have measured intensity ratios in element range $22 \leq Z \leq 69$ at 59.5 keV [14]. Ertuğrul and Şimşek have measured X-ray relative intensities of Tm, Yb, Lu, Ta, W, Re, Au, Hg, Tl, Pb, Bi, Th, and U elements [15]. Ertuğrul et al. have investigated K_{β}/K_{α} X-ray intensity

ratios for elements in the range $16 \leq Z \leq 92$ excited by photons with 5.9, 59.5, and 123.6 keV energies [16]. Dhal and Padhi have investigated relative K X-ray intensities on the elements from Mn to Sb using 59.5 keV γ -rays [17]. Chemical effects on the K_{β}/K_{α} intensity ratios and on the enhancement of the Coster-Kronig transitions have been investigated [18]. Sögüt et al. have measured an alloying effect on the intensity ratios in Cr–Ni and Cr–Al alloys [19]. Photon-excited K X-ray fluorescence cross-sections have been measured for some light elements in the range 20–60 keV by Rao et al. [20]. Krause has theoretically determined the K X-ray production cross-sections for all the elements at energies ranging from 10 to 60 keV [21]. Our earlier study is related to measurements of K -shell X-ray production cross-sections and fluorescence yields for some elements in the atomic number range $28 \leq Z \leq 40$ using secondary method [22]. K shell X-ray fluorescence cross-sections have been measured for some elements [23–25]. Özdemir et al. have investigated K X-ray intensity ratios of some $4d$ transition metals depending on the temperature [26]. K and L X-ray production cross-sections and intensity ratios of rare-earth elements for proton impact in the energy range of 20–25 MeV were reported by Hajivaliei et al. [27]. Also, there are important theoretical estimates based on relativistic Hartree-Fock and Hartree-Slater theories calculated by Scofield [28, 29].

In this work, we reported the measurements of the X-ray production cross-sections and the X-ray intensity ratios for Cr, Mn, Fe, and Co by 8.735 keV photons using secondary excitation method.

2. Experimental procedure and calculations

The experimental setup is shown in Fig. 1. In this work, the measurements have been carried out for Cr, Mn, Fe, and Co elements. The purity of commercially obtained materials was about 99%. Powder samples were sieved to 400 mesh size. The samples were irradiated by 16.896 keV excitation energy using secondary source. K X-rays emitted by samples have been counted by a Si (Li)

*e-mail: ryilmaz@yyu.edu.tr

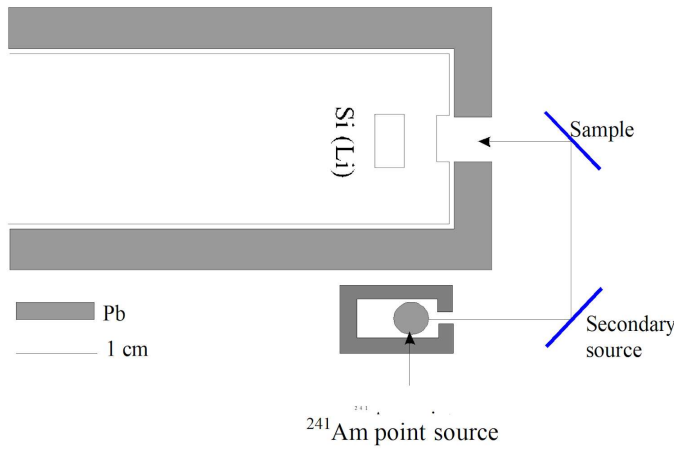


Fig. 1. Experimental setup.

detector with 160 eV resolutions at 5.9 keV. The samples were excited by the K X-rays of secondary source excited at 59.5 keV γ - rays from a ^{241}Am point source. Fluorescent X-rays spectra were recorded by a calibrated Si (Li) X-ray spectrometer (FWHM = 160 eV at 5.96 keV, active area = 12.5 mm², sensitivity depth = 3.5 cm, Be window thickness = 12.5 μm) coupled to a Nuclear Data MCA system (ND66B) consisting of a 4096-channel analyzer and spectroscopy amplifier. The net peak areas of the K X-rays of each target were determined after background subtraction, tallying and escape-peak corrections. The secondary excitation source was pure Zn (99.99%). The excitation energy was taken as the average of K_{α} and K_{β} X-ray energies. For Zn, weighted averages $K_{\alpha\beta}$ energy is 8.735 keV [30].

The intensity ratio values of the K X-rays are given by [16]:

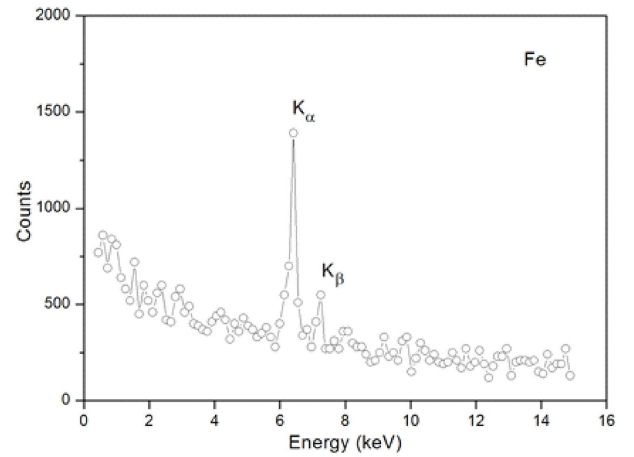
$$\frac{I(K_{\beta})}{I(K_{\alpha})} = \frac{N_{K_{\beta}} \beta_{K_{\alpha}} \varepsilon_{K_{\alpha}}}{N_{K_{\alpha}} \beta_{K_{\beta}} \varepsilon_{K_{\beta}}}, \quad (1)$$

where $N_{K_{\beta}}/N_{K_{\alpha}}$ is the ratio of the counting rates under the K_{α} and K_{β} peaks, $\beta_{K_{\alpha}}/\beta_{K_{\beta}}$ the ratio of the self-absorption correction factor of target, and $\varepsilon_{K_{\alpha}}/\varepsilon_{K_{\beta}}$ the ratio of the detector efficiency for K_{α} and K_{β} X-rays. A typical K X-ray spectrum for Fe is shown in Fig. 2.

The K -shell X-ray production cross-sections ($\sigma_{K_{\alpha}}$ and $\sigma_{K_{\beta}}$) required for the determination of K_{β}/K_{α} intensity ratios were evaluated by measuring the characteristic K X-ray intensities for cited range of elements. The experimental K X-ray production cross-sections were measured using the following relation:

$$\sigma_{K_i} = \frac{N_{K_i}}{I_0 G \varepsilon_{K_i} \beta t}, \quad (2)$$

where N_{K_i} ($i = \alpha, \beta$) is the number of counts per unit time under the corresponding photo peak. I_0 is the intensity of exciting radiation, G is the geometrical factor, ε_{K_i} is the detector efficiency for the K_i X-rays, t is the mass of the sample in g/cm² and β is the self-absorption

Fig. 2. Typical K X-ray spectrum of Fe.

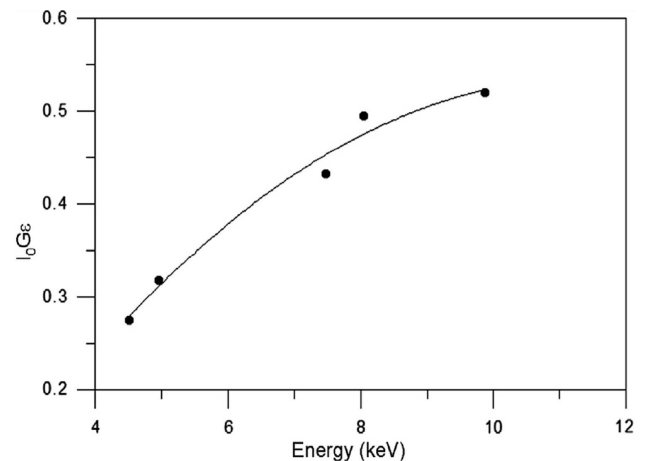
correction factor for the incident photons and emitted K X-ray photons. β is calculated by using the relation [16]:

$$\beta = \frac{1 - \exp[-(\mu_1/\sin\theta + \mu_2/\sin\theta)t]}{(\mu_1/\sin\theta + \mu_2/\sin\theta)t}, \quad (3)$$

where μ_1 and μ_2 are the absorption coefficients (cm²/g) of incident photons and emitted characteristic X-rays, respectively [31]. The angle of incident photons and emitted X-rays, with respect to the normal at the surface of the sample, θ was equal to 45° in the present setup. In the present study, as shown in Fig. 1, the values of the factors $I_0 \varepsilon G$, which contain terms related to the incident photon flux, the efficiency of the X-ray detector and geometrical factor, were determined by collecting the K X-ray spectra of thin samples of Ti, V, Ni, Cu, and Ga in the same geometry in which the K X-ray fluorescence cross-sections were measured and using Eq. (4). Also, the efficiency curve at 8.735 keV was given in Fig. 3.

$$I_0 G \varepsilon_{K_i} = \frac{N_{K_i}}{\sigma_{K_i} \beta t}. \quad (4)$$

N_{K_i} , β and t were given in Eq. (2).

Fig. 3. $I_0 \varepsilon G$ values versus K X-ray energy.

3. Theoretical method

The theoretical values of K X-ray production cross-sections $\sigma_{K\alpha}$ and $\sigma_{K\beta}$ have been calculated using the following equations [23]:

$$\sigma_{K\alpha} = \sigma_K^p(E)\omega_K f_{K\alpha}, \tag{5}$$

$$\sigma_{K\beta} = \sigma_K^p(E)\omega_K f_{K\beta}, \tag{6}$$

where $\sigma_K^p(E)$ is the K -shell photoionization cross-section for the given element at excitation energy E , ω_K is the K -shell fluorescence yield and $f_{K\alpha}$ and $f_{K\beta}$ are fractional X-ray emission rates for K_α and K_β X-rays and are defined as [32]:

$$f_{K\alpha} = (1 + I_{K\beta}/I_{K\alpha})^{-1}, \tag{7}$$

$$f_{K\beta} = (1 + I_{K\beta}/I_{K\alpha})^{-1}, \tag{8}$$

where $I_{K\beta}/I_{K\alpha}$ is the K_β to K_α X-ray intensity ratios. In the present calculations, the values of $\sigma_K^p(E)$ were taken from the Scofield based on Hartree–Slater potential theory [33], and the values of ω_K were taken from the tables of Krause [21].

4. Results and discussion

The measured values of K_α and K_β X-ray production cross-sections and K_β/K_α X-ray intensity ratios for Cr, Mn, Fe, and Co by 8.735 keV photons using secondary excitation method are listed in Tables I–III, respectively, with the theoretical and other experimental values. The overall error in the present measurements is estimated to be $<8\%$. This error is the quadrature sum of the uncertainties in the different parameters used to deduce K X-ray production cross-sections, namely, the error in the area evaluation under the K_α and K_β X-ray peak (2%), in the self-absorption correction factor ratio ($<1\%$), the product $I_0\varepsilon G$ (5%) and the other error in the non-uniform thickness ($<1\%$). In this work, in order to reduce the absorption, thin samples were also

used as the target; furthermore, an absorption correction was also performed for each sample. In order to reduce the statistical error, the spectra were recorded and about 5000–6000 counts were collected under the K_α and K_β peaks. These values have been plotted as a function of the atomic number as shown in Fig. 4 and Fig. 5.

TABLE I

Experimental and theoretical K_α X-ray cross-sections [cm^2/g].

Element	Excitation energy [keV]	Present work	Theoretical predictions
^{24}Cr	8.735	42.143 \pm 3.30	43.289
^{25}Mn	8.735	52.938 \pm 3.90	52.356
^{26}Fe	8.735	63.180 \pm 4.29	64.474
^{27}Co	8.735	76.408 \pm 5.10	75.172

TABLE II

Experimental and theoretical K_β X-ray cross-sections [cm^2/g].

Element	Excitation energy [keV]	Present work	Theoretical predictions
^{24}Cr	8.735	4.816 \pm 0.36	4.990
^{25}Mn	8.735	6.380 \pm 0.41	6.256
^{26}Fe	8.735	7.567 \pm 0.49	7.783
^{27}Co	8.735	9.254 \pm 0.55	9.152

TABLE III

The K_β/K_α intensity ratios. A — Polasik [4] (according to Coulomb gauge), B — Polasik [4] (according to Babushkin gauge).

Element	Present exp.	Calculated	A	B
^{24}Cr	0.1142 \pm 0.008	0.1152	0.1295	0.1317
^{25}Mn	0.1205 \pm 0.006	0.1194	0.1307	0.1326
^{26}Fe	0.1197 \pm 0.007	0.1207	0.1317	0.1334
^{27}Co	0.1211 \pm 0.009	0.1217	0.1326	0.1340

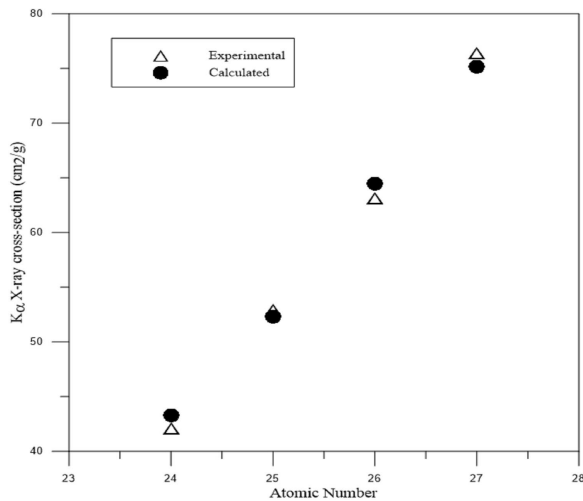


Fig. 4. Experimental and theoretical K_α X-ray cross-sections versus atomic number.

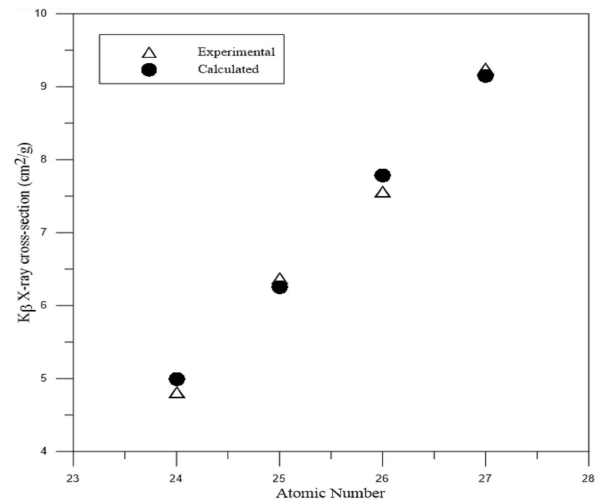


Fig. 5. Experimental and theoretical K_β X-ray cross-sections versus atomic number.

These experimental K_{β}/K_{α} X-ray intensity ratios for Cr, Mn, Fe, and Co have been compared with theoretical estimates based on MCDF calculations of Polasik [4]. These values have been plotted as a function of the atomic number as shown in Fig. 6. Our experimental values agree to within 8–13% of the K_{β}/K_{α} intensity ratios obtained using the Coulomb and Babushkin gauges of Polasik.

In conclusion, the present agreement between the theoretical and present experimental values leads to the conclusion that the data presented here will benefit those using the radioisotope XRF technique because of their application area.

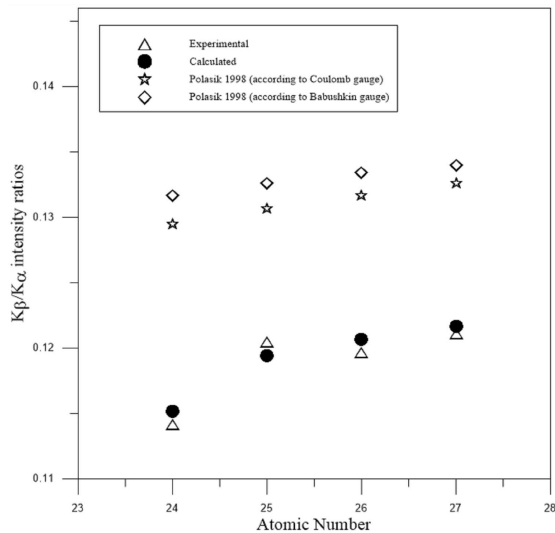


Fig. 6. K_{β}/K_{α} intensity ratios versus atomic number. Present experimental results are compared against the theoretical ones.

References

[1] M. Polasik, *Phys. Rev. A* **40**, 4361 (1989).
 [2] M. Polasik, *Phys. Rev. A* **41**, 3689 (1990).
 [3] M. Polasik, *Phys. Rev. A* **52**, 227 (1995).
 [4] M. Polasik, *Phys. Rev. A* **58**, 1840 (1998).
 [5] F.A. Babushkin, *Opt. Spektrosk.* **13**, 141 (1962).
 [6] F.A. Babushkin, *Acta Phys. Pol.* **25**, 749 (1964).
 [7] S. Raj, B.B. Dhal, H.C. Padhi, *Phys. Rev. B* **58**, 9025 (1998).
 [8] S. Raj, H.C. Padhi, M. Polasik, *Nucl. Instrum. Methods Phys. Res. B* **145**, 485 (1998).

[9] S. Raj, H.C. Padhi, D.K. Basa, M. Polasik, F. Pawlowski, *Nucl. Instrum. Methods Phys. Res. B* **152**, 417 (1999).
 [10] S. Raj, H.C. Padhi, M. Polasik, *Nucl. Instrum. Methods Phys. Res. B* **155**, 143 (1999).
 [11] S. Raj, H.C. Padhi, M. Polasik, *Nucl. Instrum. Methods Phys. Res. B* **160**, 443 (2000).
 [12] S. Raj, H.C. Padhi, *Phys. Rev. B* **63**, 073109 (2001).
 [13] F. Pawlowski, M. Polasik, S. Raj, H.C. Padhi, D.K. Basa, *Nucl. Instrum. Methods Phys. Res. B* **195**, 367 (2002).
 [14] M. Ertuğrul, Ö. Söğüt, Ö. Şimşek, E. Büyükkasap, *J. Phys. B* **34**, 909 (2001).
 [15] M. Ertuğrul, Ö. Şimşek, *J. Phys. B* **35**, 601 (2002).
 [16] B. Ertuğral, G. Apaydın, U. Çevik, M. Ertuğrul, A.İ. Kobyay, *Radiat. Phys. Chem.* **76**, 22 (2007).
 [17] B.B. Dhal, H.C. Padhi, *Phys. Rev. A* **50**, 1096 (1994).
 [18] A. Küçükönder, E. Büyükkasap, R. Yılmaz, Y. Şahin, *Acta Phys. Pol. A* **95**, 243 (1999).
 [19] Ö. Söğüt, E. Büyükkasap, A. Küçükönder, M. Ertuğrul, Ö. Şimşek, *Appl. Spectrosc. Rev.* **30**, 175 (1995).
 [20] D.V. Rao, R. Cesereo, G.E. Gigante, *X-ray Spectrom.* **22**, 406 (1993).
 [21] M.O. Krause, *J. Phys. Chem. Ref. Data* **8**, 307 (1979).
 [22] R. Yılmaz, H. Tunç, A. Özkartal, *Radiat. Phys. Chem.* **112**, 83 (2015).
 [23] R. Durak, S. Erzenoğlu, Y. Kurucu, Y. Şahin, *Radiat. Phys. Chem.* **51**, 45 (1998).
 [24] A. Karabulut, G. Budak, L. Demir, Y. Şahin, *Nucl. Instrum. Methods Phys. Res.* **155**, 369 (1999).
 [25] Y. Özdemir, R. Durak, E. Oz, *Radiat. Phys. Chem.* **65**, 199 (2002).
 [26] Y. Özdemir, E. Kavaz, N. Ahmadi, M. Ertuğrul, N. Ekinci, *Appl. Radiat. Isotopes* **115**, 147 (2016).
 [27] M. Hajivaliei, S. Puri, M.L. Garga, D. Mehta, A. Kumar, S.K. Chamoli, D.K. Avasthi, A. Mandal, T.K. Nandi, K.P. Singh, N. Singha, I.M. Govila, *Nucl. Instrum. Methods Phys. Res. B* **169**, 203 (2000).
 [28] J.H. Scofield, *Phys. Rev. A* **9**, 1041 (1974a).
 [29] J.H. Scofield, *At. Data Nucl. Data Tables* **14**, 121 (1974b).
 [30] J.H. Scofield, *Theoretical Photoionization Cross-Sections from 1 to 1500 keV* Report UCRL 51326, Lawrence Livermore Laboratory, 1973.
 [31] J.H. Hubbell, S.M. Seltzer, National Institute of Standard and Technology Report No. NISTIR 5632, 1995.
 [32] E. Storm, I. Israel, *Nuclear Data Tables* **A7**, 565 (1970).
 [33] N. Broll, *X Ray Spectrom.* **15**, 271 (1986).